

Quantifying demand and weather uncertainty in power system models using the m out of n bootstrap

Adriaan P Hilbers^{a,*}, David J Brayshaw^{b,c}, Axel Gandy^a

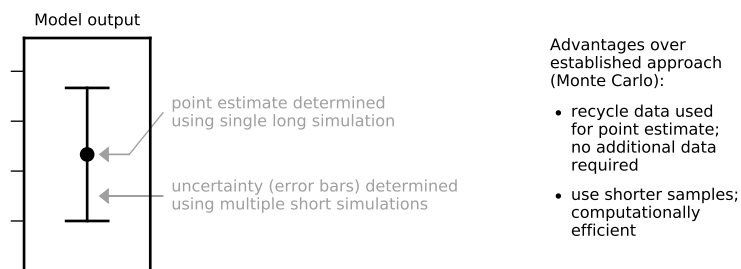
^a*Department of Mathematics, Imperial College London*

^b*Department of Meteorology, University of Reading*

^c*National Centre for Atmospheric Science, University of Reading*

Abstract

Novel approach quantifies uncertainty in computationally efficient manner without need for any additional data



This paper introduces a novel approach to quantify demand & weather uncertainty in power system models. Recent studies indicate that such sampling uncertainty, originating from demand & weather time series inputs, leads to significant uncertainties in model outputs and should not be ignored, especially with increasing levels of weather-dependent renewable generation. However, established uncertainty quantification approaches fail in this context due to the computational resources and additional data required for Monte Carlo-based analysis. The methodology introduced in this paper quantifies demand & weather uncertainty using a time series bootstrap scheme with *shorter* time series than the original, enhancing computational efficiency and avoiding the need for any additional data. It can be used both to quantify output uncertainty and to determine optimal sample lengths for prescribed confidence levels. Simulations are performed on three generation & transmission expansion planning models and a simple test is introduced allowing users to determine whether estimated uncertainty bounds are valid. Code applying the methodology to the models used in this paper is provided as open-source software.

Keywords: Power system modeling, uncertainty, time series analysis, weather

1. Introduction

1.1. Demand & weather uncertainty in power system models

Recent studies indicate that the effect of demand & weather sampling uncertainty in *power system models* (PSMs) is significant and should not be ignored. Many such models take demand & weather time series data such as hourly demand levels, wind speeds or solar irradiances as inputs (Bazmi & Zahedi, 2011; Lopion et al.,

*Corresponding author

Email address: a.hilbers17@ic.ac.uk (Adriaan P Hilbers)

2018; Ringkjøb et al., 2018). Since such inputs can be viewed as samples from some underlying distribution, associated model outputs are subject to sampling uncertainty, the magnitude of which may be significant. For example, model outputs may differ highly depending on which year of time series data is used (Bloomfield et al., 2016; Staffell, 2017; Collins et al., 2018; Zeyringer et al., 2018; Bothwell & Hobbs, 2018), with some outputs varying as much as 80% (Pfenninger, 2017; Hilbers et al., 2019). One example of the resultant difficulties is the debate between Jacobson et al. (2015) and Clack et al. (2017), partially revolving around the choice of demand & weather scenarios. This discussion shows that quantifying demand & weather uncertainty is important for robust decision-making using PSMs.

1.2. *Uncertainty quantification in PSMs: established approaches*

The power system modeling community employs a number of established techniques to quantify output uncertainty, as summarised by Kann & Weyant (2000), Soroudi & Amraee (2013) and Yue et al. (2018). Scenario analysis is convenient when considering factors that cannot reliably be described by probability distributions (e.g. future policy or the uptake speed of new technologies), while interval analysis performs well when input parameters lie between certain values and interact weakly. *Monte Carlo* methods estimate the probability distribution of outputs by running a PSM multiple times with parameter values sampled according to their respective (assumed) probability distributions. See e.g. (Pye et al., 2015; Alzbutas & Norvaisa, 2012; Fragkos et al., 2015; Bosetti et al., 2015; Hart & Jacobson, 2011) for applications to power systems.

1.3. *The m out of n and the time series bootstrap*

Since their introduction by Efron (1979), *bootstrap* methods have become popular throughout statistics and its applications. In its most basic form, the procedure emulates some output’s sampling distribution by its distribution under resampling from the available data. Its popularity is attributed to its simplicity and the fact that it “works” (referred to as its *consistency*) in a wide variety of settings (Chernick, 2007; Singh, 1981; Bickel & Freedman, 1981). The m out of n bootstrap, which uses samples of a different length (usually shorter) when calculating the bootstrap distribution, may be used to reduce computational cost. Theoretical properties, including its consistency in settings where the traditional (n out of n) bootstrap is consistent, are discussed by Bickel et al. (1997) and Bickel & Sakov (2002).

Bootstrap methods applied to time series require additional refinements when values are not independent and identically distributed (IID), as summarised by Davison & Hinkley (1997). Two common approaches are the sampling of longer blocks of timesteps to preserve short-term dependence structures (the *block bootstrap*) or the detrending of long-term dependencies and subsequent resampling of residuals (the *model-based bootstrap*).

Only few previous studies have employed bootstrap methods in energy applications. Two examples are in creating probabilistic forecasts for electricity demand (Fan & Hyndman, 2012) and residential energy use (Chiou et al., 2011).

1.4. *This paper’s contribution*

This paper introduces a new approach to quantify demand & weather sampling uncertainty in PSMs (for example, how much does a model output vary if other, but equally realistic, demand & weather samples are considered?). As discussed in Section 1.1, this uncertainty can be significant. The methods in this paper allow a user to both quantify the uncertainty’s magnitude and determine the required sample length to achieve certain confidence bounds. It hence allows a user to make robust choices without wasting computational resources.

Previous approaches to uncertainty analysis (Section 1.2) typically fail in this setting as highlighted by a simple example. Suppose a user wants uncertainty bounds on PSM outputs determined using five years of demand & weather data. Scenario or interval analysis fails due to the high dimensionality of the input data. Monte Carlo methods (running the model multiple times with different five-year demand & weather samples) are typically unfeasible due to the requirements on data (multiple five-year samples are not available) and/or computational resources (too expensive to run PSM multiple times with five-year samples). The above holds especially since accurately modeling variable renewable generation requires high temporal and spatial resolution (Poncelet et al., 2016), precluding downsampling by taking each n th time step.

The methodology presented here resolves these issues via two innovations. Samples are obtained by judicious resampling from the available data, avoiding the need for any additional data. Computational cost is reduced by using *shorter* time series and adjusting results in a statistically robust way. As a whole, the methodology is an example of the m out of n bootstrap (Section 1.3). Each of the two innovations can be used individually if only one of data availability and computational expense is limited. To the best knowledge of the authors of this paper, there exists no previous approach to quantify demand & weather sampling uncertainty in PSMs without the aforementioned issues.

The models, data and sample code applying the methodology are provided open-source at github.com/ahilbers/2020_bootstrap_uncertainty_quantification.

This paper is structured as follows. Section 2 introduces the methodology in full generality. Section 3 analyses its performance on three test-case PSMs. Section 4 discusses the results, their implications and possible extensions. A full description of the time series and employed models can be found in the appendix (Section 5).

2. Methodology

2.1. Overview

Suppose a user has demand & weather time series of length n_F indexed by time steps \mathcal{T}_F . Due to computational limitations, it may be impossible to use the full time series in a PSM run, so the user employs some subset (possibly the full time series) $\mathcal{T}_\delta \subseteq \mathcal{T}_F$ of length n_δ to determine output \hat{O} . Since all other model inputs are considered fixed, the PSM is viewed as a mapping from the time series to \hat{O} :

$$\hat{O} = \text{PSM}(\mathcal{T}_\delta). \quad (1)$$

Uncertainty in the value of \hat{O} is induced from the demand & weather time series to calculate it. In particular, a different sample of demand & weather data, drawn from the same underlying distribution as \mathcal{T}_δ is drawn from, would lead to a different but equally valid estimate \hat{O} . This is referred to as *demand & weather sampling uncertainty* on \hat{O} . In the rest of this paper, the word *sampling* is dropped and the term *demand & weather uncertainty* is used.

A convenient quantification of the demand & weather uncertainty on \hat{O} is provided by its *sampling standard deviation* σ_δ . This is \hat{O} 's standard deviation across different demand & weather data samples of length n_δ drawn from the same underlying distribution. For example, in the case $n_\delta=5$ years, such samples may be independent 5-year samples of demand & weather data. In many settings, σ_δ cannot be estimated by direct Monte Carlo analysis due to limitations in computational resources and data availability (Section 1.4). It may be estimated instead using the *bootstrap uncertainty quantification* (BUQ) algorithm.

Algorithm: *Bootstrap uncertainty quantification* (BUQ)

1. Construct K subsamples $\mathcal{S}_1, \dots, \mathcal{S}_K \subset \mathcal{T}_F$ of time steps, each of length $n_S \leq n_{\hat{O}}$, using a suitable bootstrapping procedure (discussed below).
2. For each sample, calculate output $O_k = \text{PSM}(\mathcal{S}_k)$.
3. Calculate (unbiased) estimate of the variance σ_S^2 across subsamples:

$$\sigma_S^2 = \frac{1}{K-1} \sum_{k=1}^K (O_k - \overline{O_S})^2 \quad (2)$$

where $\overline{O_S} = \frac{1}{K} \sum_{k=1}^K O_k$ is the sample mean.

4. Estimate $\sigma_{\hat{O}}$ by $\widehat{\sigma}_{\hat{O}}$, defined by

$$\widehat{\sigma}_{\hat{O}}^2 = \frac{n_S}{n_{\hat{O}}} \sigma_S^2. \quad (3)$$

The methodology also determines the required sample length $n_{\hat{O}}$ to attain uncertainty bounds. Given a required standard deviation $\widehat{\sigma}_{\hat{O}}$, (3) may be rearranged to give

$$n_{\hat{O}} = n_S \frac{\widehat{\sigma}_S^2}{\widehat{\sigma}_{\hat{O}}^2} \quad (4)$$

which gives (an estimate of) the minimum sample length required to ensure model output \hat{O} has standard deviation at most $\widehat{\sigma}_{\hat{O}}$.

The procedure in step 1 creates subsamples by bootstrapping coherent blocks of time steps while respecting seasonalities. An example is creating a 56-day sample using 2 randomly selected weeks from each of the 4 seasons. Sampling is done with replacement (so that the same week may appear twice). Precise details (e.g. the block length) may be tailored to the specific application as in Section 3.2.

2.2. *Justification and a test for validity*

The BUQ algorithm is an example of the m out of n time series bootstrap with $n = n_{\hat{O}}, m = n_S$. From bootstrap theory (Section 1.3), $\widehat{\sigma}_{\hat{O}}$ is known to approximate $\sigma_{\hat{O}}$ well in many settings provided that n_S and $n_{\hat{O}}$ are large enough and the sampled blocks are long enough to capture the autocorrelation present in the time series. The $\frac{n_S}{n_{\hat{O}}}$ scaling appears because the variance of a large class of statistical estimators (including the sample mean and medians, as well as arbitrary functions of them under weak conditions) have variances that are inversely proportional to sample size (Bickel et al., 1997; Van der Vaart, 2007).

There are two important examples in which the BUQ algorithm is not expected to provide consistent estimates. Bootstrap consistency typically relies on the target output being continuous under weak convergence. For PSMs, this requirement usually fails in one of two situations. The first is when a PSM output depends on a sample minimum or maximum, as is the case when 100% of demand must be met. This can be alleviated by allowing unmet demand at high cost, which changes the dependence on the sample maximum to a high quantile, e.g. 99.5%. The second is when the PSM output is an integer variable with jumps that are too big to be approximated well by a continuous variable.

Given some PSM output, a simple test may be used to indicate whether the BUQ algorithm provides consistent standard deviation estimates. It works as follows: repeat steps 1-4 of the BUQ algorithm with an even shorter sample length $n_Q < n_S$. If the associated variance estimates satisfy $\sigma_S^2 \approx \frac{n_S}{n_Q} \sigma_Q^2$, then the variance is decreasing

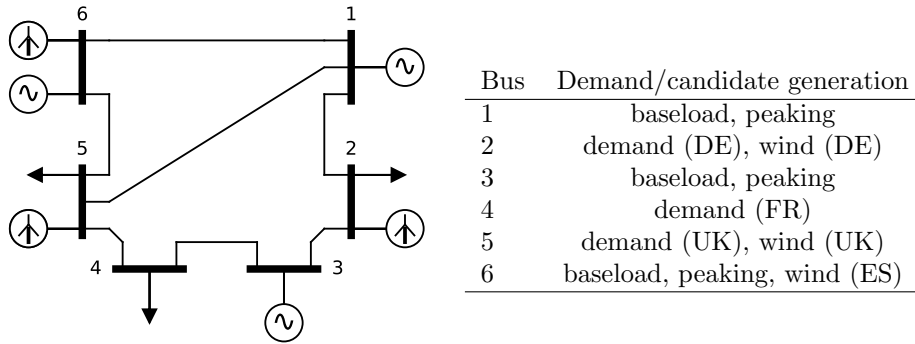


Figure 1: 6-bus model configuration. Demand must be met at buses 2, 5 and 6. Conventional generation (baseload or peaking) may be installed at buses 1, 3 and 6. Wind generation may be installed at buses 2, 5 and 6. Buses 2, 4, 5 and 6 use (demand or wind) time series data from Germany (DE), France (FR), the United Kingdom (UK) and Spain (ES) respectively.

by the required linear factor $\frac{n_Q}{n_S}$. While not a rigorous proof, satisfaction of this test is a good indicator that the estimate of $\sigma_{\hat{O}}$ is also valid.

3. Simulation results

3.1. Overview

In this section the BUQ algorithm is applied to three test PSMs. Time series inputs are hourly demand levels and wind capacity factors in European countries over the 38-year period from 1980 to 2017. Model outputs consist of the minimum “build-from-scratch” power system cost as well as the associated carbon emissions, generation capacities and generation levels. The goal is to estimate each output’s standard deviation using the BUQ algorithm introduced in Section 2. The models are not intended to be realistic representation of existing power systems but serve as test cases containing many features of real power grids.

The remainder of this section is structured as follows. Section 3.1 introduces the three test-case PSMs. Section 3.2 discusses the subsampling scheme used to make bootstrap samples in step 1 of the BUQ algorithm (Section 2.1). Section 3.3 provides evidence for the methodology’s accuracy. Section 3.4 provides a case study of application of the BUQ algorithm in four settings.

3.1.1. Model 1: 1-region LP

The *1-region LP* model is a simple linear programming (LP)-based generation expansion planning (GEP) model with a choice of three possible generation technologies: *baseload*, *peaking* and *wind*. Unmet demand (or, equivalently, load shedding) is allowed at high cost. The model takes two input time series: hourly demand levels and wind capacity factors for the United Kingdom. Section 5.1.1 describes the precise mathematical optimisation problem.

3.1.2. Model 2: 6-region LP

The *6-region LP* is a more complicated multi-region generation & transmission expansion planning (GEP/TEP) problem. The same technologies (baseload, peaking and wind) as in the *1-region LP* are permitted, and unmet demand/load shedding is allowed at high cost. The system’s 6-region topology is based on the *IEEE 6-bus system*, see e.g. (Rau & Yih-Heui Wan, 1994; Roh et al., 2009; Chen & Wu, 2015; Baharvandi et al., 2018). The available technologies at each bus are based on a

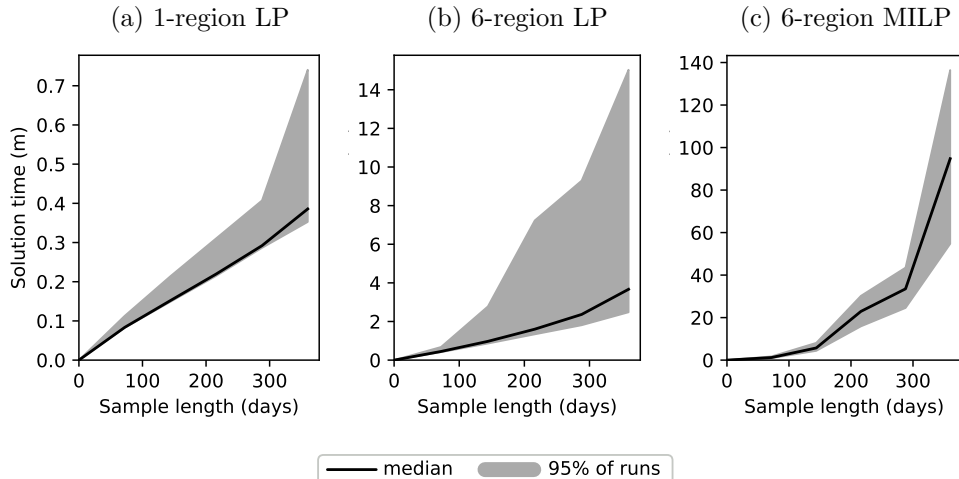


Figure 2: Distribution (across 80 runs) of computational cost required to solve each of the 3 test PSMs as a function of sample size. The black line shows the median and the grey region indicates a 95% symmetric prediction interval.

renewables-ready version of the 6-bus system introduced by Kamalinia & Shahidehpour (2010) and Kamalinia et al. (2011). Figure 1 provides a diagram of the model configuration. Full mathematical details of the model are provided in Section 5.1.2.

The *6-region LP* model returns a larger number of outputs than the *1-region LP* since each output is at regional level (e.g. baseload in regions 1, 3 and 6) and transmission expansion is also considered. This induces nonuniqueness in the solution; for example, in the case of residual demand in region 2, the optimal solution has no preference in meeting this from extra generation and transmission from region 1 versus 3. This property can be removed by considering distinct technologies at each region. However, in the interest of simplicity, this investigation concentrates on model-wide outputs (e.g. total baseload capacity), which are unique given identical input data.

3.1.3. Model 3: 6-region MILP

The *6-region MILP* model is identical to the *6-region LP* model with added integer and ramping constraints. Baseload generation capacity may be installed in blocks of 3GW (roughly a large nuclear plant) and is subject to a ramp rate of 20%/hr. The optimisation problem is hence a mixed integer linear program (MILP) with ramping constraints. Mathematica details are provided in Section 5.1.3.

3.1.4. Computational cost and time series length

Figure 2 shows the distribution of the computing time to solve each model’s optimisation problem as a function of the input demand & weather time series length. For the *1-region LP* model, solution times scale roughly linearly and 1-year simulations take 20-40 seconds. For the *6-region LP* model, solution times are longer and scale up linearly at first but then accelerate in computational cost; a 5-year simulation (not shown) takes 1 hour, much longer than 5 times the 3-minute median for 1-year simulations. Furthermore, the range in solution times across runs using the same time series lengths is large. For the *6-region MILP* model, the integer constraints cause an exponential scaling of solution times, which roughly double for every 72-day increase in sample length. Each of the above results are based on optimisation problems created in the open-source energy modeling framework **Calliope** (Pfenninger & Pickering, 2018) and solved using the **gurobi** solver on a 2.7GHz Intel Core i5-5257U processor with 8GB of RAM.

3.2. Subsampling schemes

This section describes how the K bootstrap samples (step 1, Section 2.1) are created. These subsampled time series should be realistic. For example, random sampling of time steps is not acceptable; a time step from a morning in June should not follow one from an evening in January. More generally, the subsampling should respect the spatial and temporal dependence structures present in the time series. Equal-time dependencies (e.g. correlations in the demand levels in different regions) are respected by sampling time steps as opposed to individual time series values; if the demand in region 1 at time t is sampled, then so are all other time series values at that time. In addition, four temporal dependence structures should be respected. The demand time series contains a daily, weekly and annual cycle, as well as a short-term autocorrelation (a higher-than-average demand day is more likely to be followed by another, because of e.g. a multi-day weather event). For the wind time series, the same dependence structures exist apart from the weekly cycle.

Two subsampling schemes are proposed. For the *1-region LP* and *6-region LP* model, the computational cost for multi-year simulations is not prohibitive. For the *6-region MILP* model, however, single-year simulations require around two hours and a two-year simulation is expected to require 32 times more. In this setting, multiple multi-year simulations are computationally unfeasible. For this reason, for the *1-region LP* and *6-region LP* models, a *months* block bootstrapping scheme is employed, while for the *6-region MILP* model a *weeks* scheme is used. These schemes work as follows:

- **Months:** sample individual months, correctly distributed throughout the year. For example, a 2-year sample is as follows:

$$[\text{Jan}][\text{Feb}] \cdots [\text{Nov}][\text{Dec}][\text{Jan}][\text{Feb}] \cdots [\text{Nov}][\text{Dec}] \quad (5)$$

where [Jan] is a contiguous January block from one of the 38 January months (from 1980 to 2017) and other blocks are defined similarly.

- **Weeks:** sample individual weeks, correctly distributed throughout the (meteorological) seasons. For example, a 56-day sample is as follows:

$$[7\text{d}]_{\text{DJF}}[7\text{d}]_{\text{MAM}}[7\text{d}]_{\text{JJA}}[7\text{d}]_{\text{SON}}[7\text{d}]_{\text{DJF}}[7\text{d}]_{\text{MAM}}[7\text{d}]_{\text{JJA}}[7\text{d}]_{\text{SON}} \quad (6)$$

where $[7\text{d}]_{\text{DJF}}$ is a contiguous week block from one of the meteorological winters (Dec-Jan-Feb) present in the 38-year time series and the other blocks are defined similarly for the other seasons.

Note that daily, weekly and seasonal cycles are preserved by design, and the short-term autocorrelation is preserved provided the length of this dependence is shorter than the block length (1 month and 7 days respectively).

3.3. Verifying the methodology's consistency

In this section, the methodology's consistency is considered. Suppose a user seeks the standard deviation of model output \hat{O} obtained using a single-year simulation. This can be estimated in two ways. The first is across the 38 individual years (1980-2017) of data, which provides a rough estimate for the standard deviation across "real" 1-year samples drawn from the underlying demand & weather distribution. The second is with the BUQ algorithm (Section 2.1) with some subsample length n_S .

If the methodology is consistent, one expects that the BUQ estimate is close to that found using individual years. This indicates that the BUQ algorithm (which uses *bootstrap* samples) approximates the standard deviation across "real" samples drawn from the underlying distribution. Furthermore, the BUQ estimate should be independent of n_S provided that n_S is not too small. This indicates that the $\frac{n_S}{n_O}$ factor

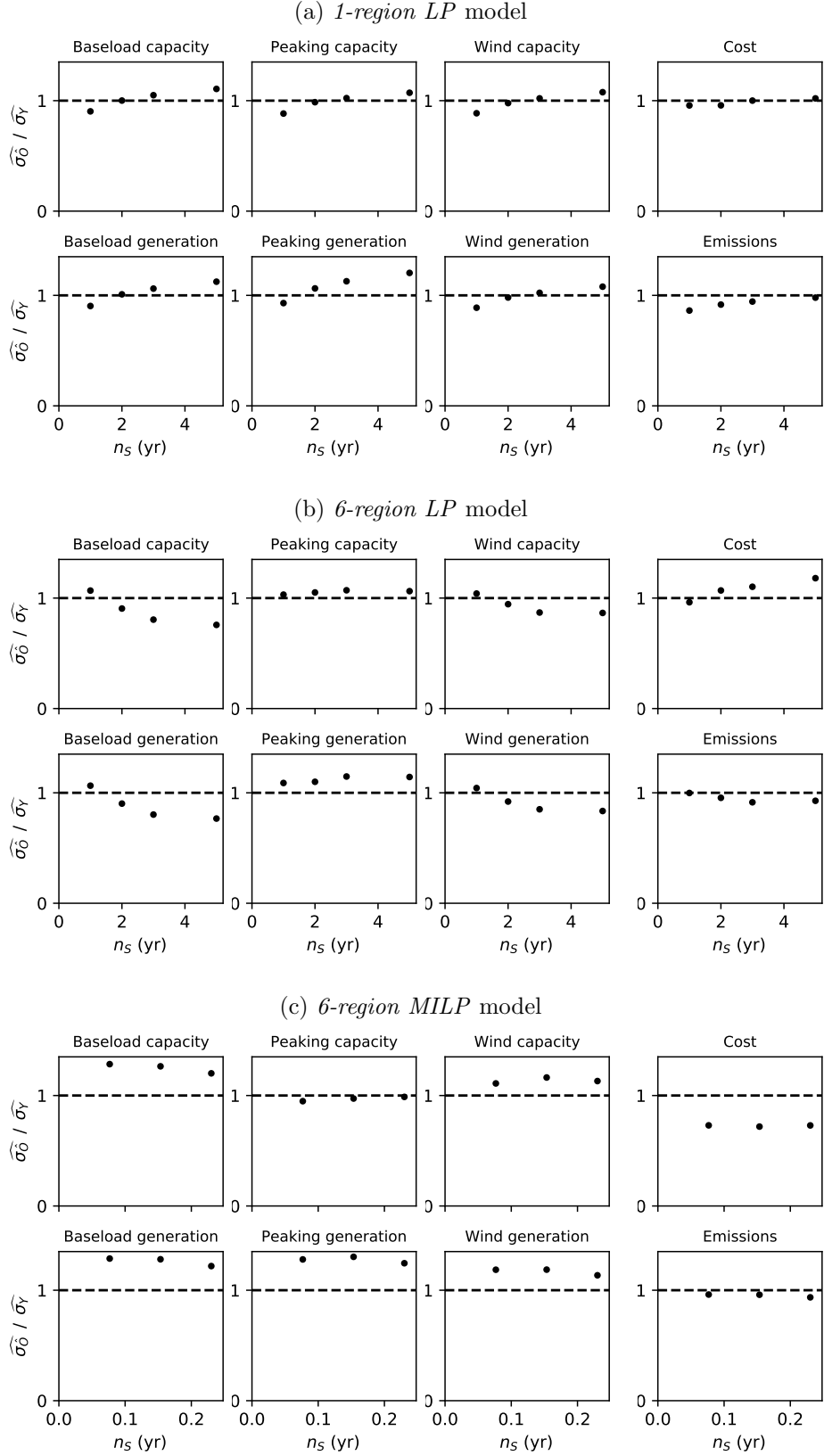


Figure 3: BUQ standard deviation estimates $\widehat{\sigma}_O$ as a function of sample size n_S . The standard deviation is calculated across $K=1000$ bootstrap samples, generated by the *months* scheme for the *1-region LP* and *6-region LP* models and the *weeks* scheme for the *6-region MILP* model. The dashed line shows $\widehat{\sigma}_Y$, the variance across the 38 individual years from 1980-2018. The y value is shown as a proportion of $\widehat{\sigma}_Y$.

	model	\hat{O} (point estimate)			$\hat{\sigma}_O$ (stand. dev. estimate)		
		$n_{\hat{O}}$	sample	solution time	n_S	subsample scheme	solution time per run
(a)	1-region LP	38yr	1980-2017	27min	38yr	months	30min
(b)	6-region LP	10yr	2008-2017	391min	1yr	months	4min
(c)	6-region LP	1yr	2017	4min	1yr	months	4min
(d)	6-region MILP	1yr	2017	122min	4wk	weeks	<1min

Table 1: Samples used to generate point estimate \hat{O} and standard deviation estimate $\hat{\sigma}_O$ in Section 3.4. For $\hat{\sigma}_O$, the mean solution time per run is shown. All subsamples are drawn from the full 38-year time series.

used in step 4 of the algorithm (Section 2.1) appropriately corrects for the change in sample length.

Figure 3 shows the BUQ standard deviation estimates $\hat{\sigma}_O$ as a function of the sample size n_S used to calculate them. For the *1-region LP* and *6-region LP* models, bootstrap samples are created using the *months* scheme for lengths $n_S=1, 2, 3$ and 5 years. For the *6-region MILP*, bootstrap samples are created using the *weeks* scheme for lengths $n_S=4, 8$ and 12 weeks. The standard deviation across individual years is shown as a dashed line.

In Figure 3, all estimates are close together as required, with a maximum error of around $\pm 15\%$ across all plots. Some error in the y -value of the dashed line is expected since it is calculated using just 38 samples, and this could explain the error between the line and dots in Figure 3(c). Hence, the behavior seen in this setting is consistent with the BUQ algorithm “working”.

3.4. Estimating the standard deviation

This section illustrates a concrete application of the BUQ algorithm in four test cases. In each test case, a single long simulation provides a point estimate \hat{O} for each model output. Estimates for the associated sampling standard deviation are generated from the BUQ algorithm (Section 2.1) with $K=1000$ bootstrap samples.

Table 1 provides details of each test case, labelled (a)-(d). Test case (a) uses the *1-region LP* model, for which computational cost is not prohibitive and all 38 years of available data are used to determine \hat{O} , followed by bootstrap samples of the same length to estimate σ_O . This corresponds to a “traditional” block bootstrap without any change in sample length. Test case (b) uses the *6-region LP* model, for which computational cost precludes a 38-year simulation. Here, bootstrap runs of length one year are used to estimate the standard deviation on \hat{O} determined using the latest ten years of data. Test case (c) repeats this experiment, but with a point estimate based on just one year of data instead of ten. This is done to highlight more explicitly the relationship between sample length and standard deviation through comparison with (b). Test case (d) uses the *6-region MILP* model. Since computational cost scales quickly with time series length for this model, four-week runs are used to estimate the standard deviation of outputs from a one-year simulation.

Figures 4(a)-(d) show, for each of the four test cases, the point estimates \hat{O} with error bars of length $2\sigma_O$ above and below. For test case (a), the use of a long 38-year sample for the point estimate means that uncertainty levels are very small. This is to be expected, since the 38-year time series encompasses much of the demand & weather variability. In test case (b), $2\sigma_O$ is around 5% for installed capacities and generation levels but is much smaller for system cost and emissions. In test case (c), the use of a short sample for the point estimate leads to significant uncertainty levels. For example, a decision-maker could not say with any certainty whether it is optimal to build more baseload capacity than wind, since the error bars overlap considerably. The same is true for test case (d).

Comparing test cases (a)-(d) highlight some key messages. Firstly, a comparison between (b) and (c) is a clear illustration of the relationship between standard

deviation and sample length. By equation (4), the standard deviation scales with inverse square root sample length, meaning the error bars in test case (c) are $\sqrt{10} \approx 3$ bigger than in (b). Furthermore, the test cases corroborate the results of previous studies (Section 1.1) that highlight the risk is using short demand & weather samples in power system modeling. For example, single-year simulations lead to large uncertainty bounds, meaning robust decision-making is difficult. Additionally, in all test cases, the uncertainty in optimal cost is small when compared to other outputs, a conclusion also found by Bothwell & Hobbs (2018) and discussed by Hilbers et al. (2019). Finally, the point estimates in test cases (b), (c) and (d) are all very close. For (b) and (c), this is purely coincidence: the 2017 outputs happened to be close to the 10-year ones, but this is not true for other years. Test cases (c) and (d), on the other hand, are similar because the integer jumps and ramping constraints in the *6-region MILP* model are weak enough that output are well approximated by the continuous analog.

4. Discussion

4.1. Context & contribution

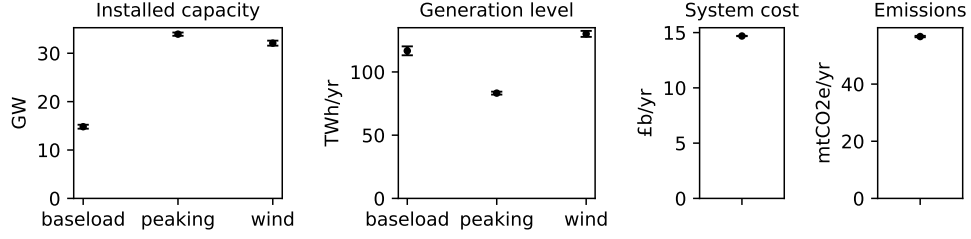
As discussed in Section 1.1, the effect of demand & weather sampling uncertainty in power system modelling should not be ignored, and quantifying its magnitude is important for robust decision-making. However, established uncertainty analysis approaches as discussed in Section 1.2 typically fail in this setting due to limitations in data availability and computational resources. This paper introduces a new methodology to quantify such uncertainty that avoids these pitfalls by block bootstrapping shorter time series sampled from the data already available. Resultant uncertainty estimates provide an information advantage over point estimates by indicating whether a model output is a statistically robust or an artifact of the particular choice of demand & weather sample. Furthermore, the methodology provides a way to inform simulation lengths by picking, using equation (4), the shortest length that leads to a desired level of certainty. Though not discussed here, confidence intervals follow the same scaling. This allows an informed choice and avoids wasting computational resources: a simulation length may be picked as short as possible and any spare resources may be used to e.g. increase model detail.

Section 3.4 highlights the advantages of the introduced methodology. For test cases (a), (b) and (d), quantifying demand & weather sampling uncertainty by established approaches (Section 1.2) is impossible. For test case (a), this would require additional 38-year data samples, which are not available. For test case (b), both data availability (many ten-year samples required) and computational cost (many ten-year simulations) are prohibitive. For test case (d), the same problems occur. The fact that it is possible to use $K=1000$ bootstrap samples (leading to stable standard deviation estimates) highlights the efficiency of the BUQ algorithm in both data and computational resources.

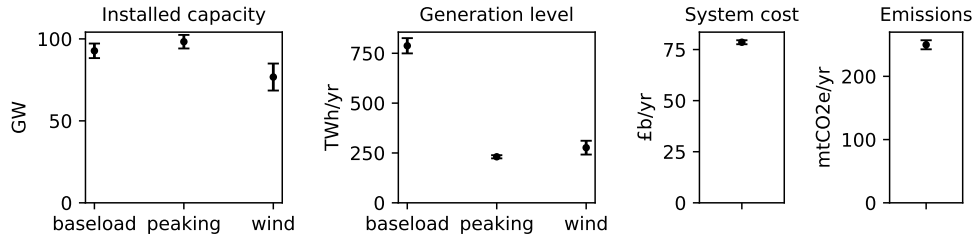
The methodology can be expected to “work” (give accurate uncertainty estimates) for most PSM outputs. Two notable exceptions are when the model output depends on a sample maximum (e.g. required peaking capacity when 100% of demand must always be met) and when the output is a discontinuous variable with steps too large to be reasonably approximated by a continuous one. In the simulations run in this paper (Section 3), this is not a problem since unmet demand is allowed and the solutions to the *6-region MILP* model were close to the associated continuous *6-region LP*. When a user is unsure whether the proposed bootstrapping scheme will “work”, a simple test – verifying that the standard deviation estimates across an even shorter sample length gives a similar estimate – gives a reasonable indication whether this is the case.

The results in this paper also provide another warning against the use of short demand & weather samples in PSMs (see Section 1.1). For the model considered, the

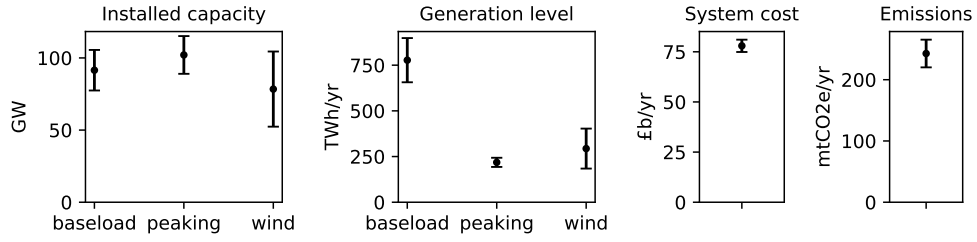
(a) 1-region LP model, $n_{\hat{O}}=38\text{yr}$, $n_S=38\text{yr}$



(b) 6-region LP model, $n_{\hat{O}}=10\text{yr}$, $n_S=1\text{yr}$



(c) 6-region LP model, $n_{\hat{O}}=1\text{yr}$, $n_S=1\text{yr}$



(d) 6-region MILP model, $n_{\hat{O}}=1\text{yr}$, $n_S=4\text{wk}$

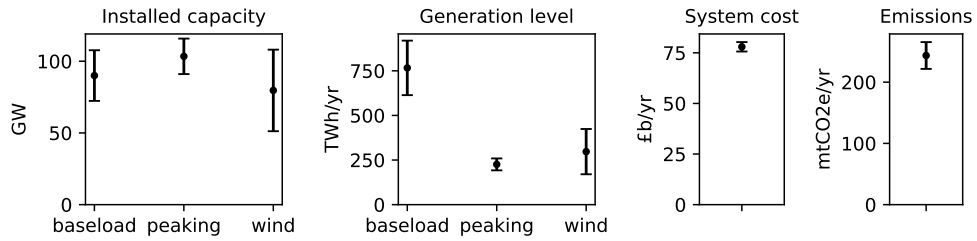


Figure 4: Estimates for value \hat{O} of model outputs, with error bars equal to $2\hat{\sigma}_{\hat{O}}$ (2 standard deviations) above and below. \hat{O} is the output of a single long simulation and $\hat{\sigma}_{\hat{O}}$ is estimated using the proposed methodology with $K=1000$ bootstrap samples. See Table 1 for details on the simulations employed.

Term	Description	Term	Description
Indices		Time series	
i	Generation technology	$d_{r,t}$	Demand, region r , time step t (GWh)
r, r'	Region	$w_{r,t}$	Wind capacity factor, region r , time t ($\in [0, 1]$)
t	Time step	Decision variables	
Sets		$\text{cap}_{i,r}^{\text{gen}}$	Generation capacity, technology i , region r (GW)
\mathcal{I}	Technologies: baseload (b), peaking (p), wind (w), unmet demand (u)	$\text{cap}_{r,r'}^{\text{tr}}$	Transmission capacity, region r to r' (GW)
\mathcal{D}	Decision variables	$\text{gen}_{i,r,t}$	Generation, technology i , region r , time t (GWh)
Parameters		$\text{tr}_{r,r',t}$	Transmission, region r to region r' , time t (GWh)
C_i^{gen}	Install cost, technology i (£m/GWyr)		
$C_{r,r'}^{\text{tr}}$	Install cost, transmission, region r to r' (£m/GWyr)		
F_i^{gen}	Generation cost, technology i (£m/GWh)		

Table 2: Nomenclature.

$\hat{O} \pm 2\sigma$ region for optimal wind capacity extends roughly 40% in each direction. A selection of four randomly sampled weeks from seasons would lead to a range of 0% to more than 200%. For robust PSM outputs, long samples (spanning multiple years) should at least be considered, although more judicious subsampling approaches (as discussed in Section 4.2) may be used to reduce sample length while introducing less uncertainty than random subsampling.

4.2. Possible extensions

One possible extension to this investigation is to combine the proposed methodology to uncertainty analysis on other model inputs (e.g. technology costs). In Monte Carlo methods, uncertain inputs may be sampled simultaneously (e.g. one time series, one fuel price and one technology cost per simulation). However, consistent use of *shorter* time series combined with other sampled inputs may require additional modifications.

Other possible extensions include uncertainty quantification for subsampled data. Due to computational limitations, PSMs are frequently run on time series subsampled from a longer one, often by clustering into representative days (de Sisternes & Webster, 2013; Nahmmacher et al., 2016; Härtel et al., 2017; Kotzur et al., 2018; Tejada-Arango et al., 2018) or by *importance subsampling* (Hilbers et al., 2019) instead of, as in this paper, a contiguous and unweighted time series. Such methodologies can be straightforwardly combined with the BUQ algorithm, by using subsampled data to obtain the point estimate and shorter contiguous time series to construct uncertainty bounds.

A final extension is the analysis of the *covariance* of model outputs. In this investigation, each model output is considered independent and each standard deviation is calculated independently. In many settings, these will vary together.

5. Appendix

5.1. Mathematical formulation of test case power system models

The three test PSMs determine outputs by solving the following optimisation problems.

5.1.1. 1-region LP

$$\min \left[\frac{T}{8760} \underbrace{\left(\sum_{i \in \mathcal{I}} C_i^{\text{gen}} \text{cap}_{i,1}^{\text{gen}} \right)}_{\substack{\text{installation cost,} \\ \text{generation capacity}}} + \underbrace{\sum_{i \in \mathcal{I}} \sum_{t=1}^T F_i^{\text{gen}} \text{gen}_{i,1,t}}_{\text{generation cost}} \right] \quad (7)$$

by optimising over decision variables

$$\mathcal{D} = \{ \text{cap}_{i,r}^{\text{gen}}, \text{gen}_{i,r,t} : i \in \mathcal{I}; t = 1 \dots T \} \quad (8)$$

subject to

$$\sum_{i \in \mathcal{I}} \text{gen}_{i,1,t} = d_{1,t} \quad \forall t \quad (9)$$

$$\text{gen}_{b,1,t} \leq \text{cap}_{b,1}^{\text{gen}} \quad \forall t \quad (10)$$

$$\text{gen}_{p,1,t} \leq \text{cap}_{p,1}^{\text{gen}} \quad \forall t \quad (11)$$

$$\text{gen}_{w,1,t} \leq \text{cap}_{w,r}^{\text{gen}} w_{1,t} \quad \forall t \quad (12)$$

$$\text{cap}_{i,1}^{\text{gen}}, \text{gen}_{i,1,t} \geq 0 \quad \forall i, t. \quad (13)$$

(9) is the demand balance requirement (allowing unmet demand). (10)-(12) ensure generation does not exceed installed capacity (for conventional technologies) or installed capacity times the wind capacity factor (for wind).

5.1.2. 6-region LP

Model 2 is identical to Model 3 without integer and ramping constraints. Hence, it solves (14)-(26) but **without** necessarily satisfying (23) and (24).

5.1.3. 6-region MILP

$$\min \sum_{r \in \mathcal{R}} \left[\frac{T}{8760} \left(\underbrace{\sum_{i \in \mathcal{I}} C_i^{\text{gen}} \text{cap}_{i,r}^{\text{gen}}}_{\substack{\text{installation cost,} \\ \text{generation capacity}}} + \frac{1}{2} \underbrace{\sum_{r' \in \mathcal{R}} C_{r,r'}^{\text{tr}} \text{cap}_{r,r'}^{\text{tr}}}_{\substack{\text{installation cost,} \\ \text{transmission capacity}}} \right) + \underbrace{\sum_{i \in \mathcal{I}} \sum_{t=1}^T F_i^{\text{gen}} \text{gen}_{i,r,t}}_{\text{generation cost}} \right] \quad (14)$$

by optimising over decision variables

$$\{ \text{cap}_{i,r}^{\text{gen}}, \text{cap}_{r,r'}^{\text{tr}}, \text{gen}_{i,r,t}, \text{tr}_{r,r',t} : i \in \mathcal{I}; r, r' \in \mathcal{R}; t = 1 \dots T \} \quad (15)$$

Technology	Installation cost (£m/GWyr)	Generation cost (£m/GWh)	Carbon emissions (t CO ₂ /GWh)
Generation technologies			
Baseload	$C_b^{\text{gen}} = 300$	$F_b^{\text{gen}} = 0.005$	$e_b = 200$
Peaking	$C_p^{\text{gen}} = 100$	$F_p^{\text{gen}} = 0.035$	$e_m = 400$
Wind	$C_w^{\text{gen}} = 100$	$F_w^{\text{gen}} = 0$	$e_w = 0$
Unmet demand	$C_u^{\text{gen}} = 0$	$F_u^{\text{gen}} = 6$	$e_u = 0$
Transmission technologies			
Regions 1 to 5	$C_{1,5}^{\text{tr}} = 150$	-	-
Other links	$C_{r,r'}^{\text{tr}} = 100$	-	-

Table 3: Costs and carbon emissions of generation and transmission technologies. Transmission costs consist only of installation costs. Installation costs are annualised so as to reflect cost per year of plant lifetime.

subject to

$$\text{cap}_{b,r}^{\text{gen}} \Big|_{r \neq 1,3,6} = \text{cap}_{p,r}^{\text{gen}} \Big|_{r \neq 1,3,6} = \text{cap}_{w,r}^{\text{gen}} \Big|_{r \neq 2,5,6} = 0 \quad (16)$$

$$\text{cap}_{r,r'}^{\text{tr}} \Big|_{\{r,r'\} \neq \{1,2\}, \{1,5\}, \{1,6\}, \{2,3\}, \{3,4\}, \{4,5\}, \{5,6\}} = 0 \quad (17)$$

$$\sum_{i \in \mathcal{I}} \text{gen}_{i,r,t} + \sum_{r'=1}^6 \text{tr}_{r',r,t} = d_{r,t} \quad \forall r, t \quad (18)$$

$$\text{tr}_{r,r',t} + \text{tr}_{r',r,t} = 0 \quad \forall r, r', t \quad (19)$$

$$\text{gen}_{b,r,t} \leq \text{cap}_{b,r}^{\text{gen}} \quad \forall r, t \quad (20)$$

$$\text{gen}_{p,r,t} \leq \text{cap}_{p,r}^{\text{gen}} \quad \forall r, t \quad (21)$$

$$\text{gen}_{w,r,t} \leq \text{cap}_{w,r}^{\text{gen}} w_{r,t} \quad \forall r, t \quad (22)$$

$$|\text{gen}_{b,r,t} - \text{gen}_{b,r,t+1}| \leq 0.2 \text{cap}_{b,r}^{\text{gen}} \quad \forall r, t \quad (23)$$

$$\text{cap}_{b,r}^{\text{gen}} \in 3\mathbb{Z} \quad \forall r \quad (24)$$

$$|\text{tr}_{r,r',t}| \leq \text{cap}_{r,r'}^{\text{tr}} \quad \forall r, r', t \quad (25)$$

$$\text{cap}_{i,r}^{\text{gen}}, \text{cap}_{r,r'}^{\text{tr}}, \text{gen}_{i,r,t} \geq 0 \quad \forall i, r, t. \quad (26)$$

(16)-(17) stipulate the locations of generation technologies and the model's transmission topology. (18) and (19) are the demand and power flow balance requirements. (20)-(22) ensure generation does not exceed installed capacity (for conventional technologies) or installed capacity times the wind capacity factor (for wind). (23) is the baseload ramping constraint. (24) enforces that baseload is built in 3GW units. (25) caps transmitted power at installed transmission capacity.

5.2. Generation & transmission technology characteristics

Peaking technology is based on a UK CCGT H class reactor described by (Department for Business, Energy and Industrial Strategy, 2016), with build cost £100/kW per year of plant lifetime, wholesale gas price of 2 pence per kWh, generation efficiency 55% and carbon emissions of 400 grams of CO₂ equivalent per kWh (Staffell, 2019). *Baseload* and *wind* technologies are based on the eponymous technologies in (Hilbers et al., 2019). Unmet demand is considered, for modeling purposes, a fourth technology with no installation cost but a generation cost of £6,000/MWh = £6m/GWh, used in some industrial applications as the value of lost load in the UK (Bucaj, 2018). All transmission lines have an identical install price of £100m/GW per year of plant lifetime, except the diagonal line from bus/region 1 to 5 with a 50% higher cost. Transmission through installed lines is assumed free and without energy loss.

5.3. Time series inputs

The time series are country-aggregated hourly demand levels and wind capacity factors for different European countries over the period 1980-2017. Details can be found in (Bloomfield et al., 2019).

5.4. Open-source models, data and code

The models, data and sample code applying the BUQ algorithm are provided as open-source software at github.com/ahilbers/2020_bootstrap_uncertainty_quantification.

Acknowledgements

The first author's work was funded through the EPSRC CDT in Mathematics for Planet Earth, grant number EP/L016613/1. The authors thank Hannah Bloomfield for providing demand & weather time series.

References

References

- Alzbutas, R., & Norvaisa, E. (2012). Uncertainty and sensitivity analysis for economic optimisation of new energy source in Lithuania. *Progress in Nuclear Energy*, *61*, 17 – 25. doi:10.1016/j.pnucene.2012.06.006.
- Baharvandi, A., Aghaei, J., Niknam, T., Shafie-Khah, M., Godina, R., & Catalo, J. P. S. (2018). Bundled generation and transmission planning under demand and wind generation uncertainty based on a combination of robust and stochastic optimization. *IEEE Transactions on Sustainable Energy*, *9*, 1477–1486. doi:10.1109/TSTE.2018.2789398.
- Bazmi, A., & Zahedi, G. (2011). Sustainable energy systems: Role of optimization modeling techniques in power generation and supply — a review. *Renewable and Sustainable Energy Reviews*, *15*, 3480–3500. doi:10.1016/j.rser.2011.05.003.
- Bickel, P. J., & Freedman, D. A. (1981). Some asymptotic theory for the bootstrap. *The Annals of Statistics*, *9*, 1196–1217.
- Bickel, P. J., Götze, F., & Van Zwet, W. R. (1997). Resampling fewer than n observations: gains, losses and remedies for losses. *Statistica Sinica*, *7*, 1–31. doi:10.1007/978-1-4614-1314-1_17.
- Bickel, P. J., & Sakov, A. (2002). Extrapolation and the bootstrap. *Sankhyā: The Indian Journal of Statistics, Series A (1961-2002)*, *64*, 640–652.
- Bloomfield, H. C., Brayshaw, D. J., & Charlton-Perez, A. (2019). Characterising the winter meteorological drivers of the European electricity system using targeted circulation types. *Meteorological Applications (to appear)*, . doi:10.1002/met.1858.
- Bloomfield, H. C., Brayshaw, D. J., Shaffrey, L., Coker, P., & Thornton, H. (2016). Quantifying the increasing sensitivity of power systems to climate variability. *Environmental Research Letters*, *11*, 124025. doi:10.1088/1748-9326/11/12/124025.
- Bosetti, V., Marangoni, G., Borgonovo, E., Anadon, L. D., Barron, R., McJeon, H. C., Politis, S., & Friley, P. (2015). Sensitivity to energy technology costs: A multi-model comparison analysis. *Energy Policy*, *80*, 244 – 263. doi:10.1016/j.enpol.2014.12.012.

- Bothwell, C., & Hobbs, B. F. (2018). Sensitivity of resource adequacy to sample error in systems with dependent renewable generation. In *2018 IEEE International Conference on Probabilistic Methods Applied to Power Systems (PMAPS)* (pp. 1–6). doi:10.1109/PMAPS.2018.8440524.
- Bucaj, E. (2018). *Value of lost load review process*. Technical Report. Elexon. URL: https://www.elexon.co.uk/wp-content/uploads/2017/09/33_278_10_VoLL-Review-Process-Paper-v1.0.pdf.
- Chen, Z., & Wu, L. (2015). Effective load carrying capability evaluation for high penetration renewable energy integration. In *2015 IEEE Power Energy Society General Meeting* (pp. 1–5). doi:10.1109/PESGM.2015.7286141.
- Chernick, M. R. (2007). *Bootstrap methods: a guide for practitioners and researchers*. (2nd ed.). Wiley Series in Probability and Statistics.
- Chiou, Y.-S., Carley, K. M., Davidson, C. I., & Johnson, M. P. (2011). A high spatial resolution residential energy model based on American time use survey data and the bootstrap resampling method. *Energy and Buildings*, *43*, 3528 – 3538. doi:10.1016/j.enbuild.2011.09.020.
- Clack, C. T. M., Qvist, S. A., Apt, J., Bazilian, M., Brandt, A. R., Caldeira, K., Davis, S. J., Diakov, V., Handschy, M. A., Hines, P. D. H., Jaramillo, P., Kammen, D. M., Long, J. C. S., Morgan, M. G., Reed, A., Sivaram, V., Sweeney, J., Tynan, G. R., Victor, D. G., Weyant, J. P., & Whitacre, J. F. (2017). Evaluation of a proposal for reliable low-cost grid power with 100% wind, water, and solar. *Proceedings of the National Academy of Sciences*, *114*, 6722–6727. doi:10.1073/pnas.1610381114.
- Collins, S., Deane, P., Ó Gallachóir, B., Pfenninger, S., & Staffell, I. (2018). Impacts of inter-annual wind and solar variations on the European power system. *Joule*, *2*, 2076 – 2090. doi:10.1016/j.joule.2018.06.020.
- Davison, A. C., & Hinkley, D. V. (1997). *Bootstrap methods and their applications*. (11th ed.). Cambridge University Press.
- de Sisternes, F. J., & Webster, M. D. (2013). Optimal selection of sample weeks for approximating the net load in generation planning problems. *ESD Working Papers*, (pp. 1–12).
- Department for Business, Energy and Industrial Strategy (2016). *Electricity Generation costs*. Technical report. Department for Business, Energy and Industrial Strategy.
- Efron, B. (1979). Bootstrap methods: Another look at the jackknife. *The Annals of Statistics*, *7*, 1–26. doi:10.1214/aos/1176344552.
- Fan, S., & Hyndman, R. J. (2012). Short-term load forecasting based on a semi-parametric additive model. *IEEE Transactions on Power Systems*, *27*, 134–141. doi:10.1109/TPWRS.2011.2162082.
- Fragkos, P., Kouvaritakis, N., & Capros, P. (2015). Incorporating uncertainty into world energy modelling: the PROMETHEUS model. *Environmental Modeling & Assessment*, *20*, 549 – 569. doi:10.1007/s10666-015-9442-x.
- Hart, E. K., & Jacobson, M. Z. (2011). A Monte Carlo approach to generator portfolio planning and carbon emissions assessments of systems with large penetrations of variable renewables. *Renewable Energy*, *36*, 2278 – 2286. doi:10.1016/j.renene.2011.01.015.

- Härtel, P., Kristiansen, M., & Korpås, M. (2017). Assessing the impact of sampling and clustering techniques on offshore grid expansion planning. *Energy Procedia*, *137*, 152–161. doi:10.1016/j.egypro.2017.10.342.
- Hilbers, A. P., J.Braysshaw, D., & Gandy, A. (2019). Importance subsampling: improving power system planning under climate-based uncertainty. *Applied Energy*, *251*, 113114. doi:10.1016/j.apenergy.2019.04.100.
- Jacobson, M. Z., Delucchi, M. A., Cameron, M. A., & Frew, B. A. (2015). Low-cost solution to the grid reliability problem with 100% penetration of intermittent wind, water, and solar for all purposes. *Proceedings of the National Academy of Sciences of the United States of America*, *112*, 1506015065. doi:10.1073/pnas.1510028112.
- Kamalinia, S., & Shahidehpour, M. (2010). Generation expansion planning in wind-thermal power systems. *IET Generation, Transmission & Distribution*, *4-8*, 940–951. doi:10.1049/iet-gtd.2009.0695.
- Kamalinia, S., Shahidehpour, M., & Khodaei, A. (2011). Security-constrained expansion planning of fast-response units for wind integration. *Electric Power Systems Research*, *81*, 107 – 116. doi:10.1016/j.epsr.2010.07.017.
- Kann, A., & Weyant, J. P. (2000). Approaches for performing uncertainty analysis in large-scale energy/economic policy models. *Environmental Modeling & Assessment*, *5*, 29 – 46. doi:10.1023/A:1019041023520.
- Kotzur, L., Markewitz, P., Robinius, M., & Stolten, D. (2018). Impact of different time series aggregation methods on optimal energy system design. *Renewable Energy*, *117*, 474–487. doi:10.1016/j.renene.2017.10.017.
- Lopion, P., Markewitz, P., Robinius, M., & Stolten, D. (2018). A review of current challenges and trends in energy systems modeling. *Renewable and Sustainable Energy Reviews*, *96*, 156 – 166. doi:10.1016/j.rser.2018.07.045.
- Nahmmacher, P., Schmid, E., Hirth, L., & Knopf, B. (2016). Carpe diem: a novel approach to select representative days for long-term power system modeling. *Energy*, *112*, 430–442. doi:10.1016/j.energy.2016.06.081.
- Pfenninger, S. (2017). Dealing with multiple decades of hourly wind and PV time series in energy models: a comparison of methods to reduce time resolution and the planning implications of inter-annual variability. *Applied Energy*, *197*, 1–13. doi:10.1016/j.apenergy.2017.03.051.
- Pfenninger, S., & Pickering, B. (2018). Calliope: a multi-scale energy systems modelling framework. *Journal of Open Source Software*, *3(29)*, 825. doi:10.21105/joss.00825.
- Poncelet, K., Delarue, E., Six, D., Duerinck, J., & D’haeseleer, W. (2016). Impact of the level of temporal and operational detail in energy-system planning models. *Applied Energy*, *162*, 631 – 643. doi:10.1016/j.apenergy.2015.10.100.
- Pye, S., Sabio, N., & Strachan, N. (2015). An integrated systematic analysis of uncertainties in UK energy transition pathways. *Energy Policy*, *87*, 673–684. doi:10.1016/j.enpol.2014.12.031.
- Rau, N. S., & Yih-Heui Wan (1994). Optimum location of resources in distributed planning. *IEEE Transactions on Power Systems*, *9*, 2014–2020. doi:10.1109/59.331463.

- Ringkjøb, H.-K., Haugan, P. M., & Solbrekke, I. M. (2018). A review of modelling tools for energy and electricity systems with large shares of variable renewables. *Renewable and Sustainable Energy Reviews*, *96*, 440 – 459. doi:10.1016/j.rser.2018.08.002.
- Roh, J. H., Shahidehpour, M., & Wu, L. (2009). Market-based generation and transmission planning with uncertainties. *IEEE Transactions on Power Systems*, *24*, 1587–1598. doi:10.1109/TPWRS.2009.2022982.
- Singh, K. (1981). On the asymptotic accuracy of Efron’s bootstrap. *The Annals of Statistics*, *9*, 1187–1195.
- Soroudi, A., & Amraee, T. (2013). Decision making under uncertainty in energy systems: State of the art. *Renewable and Sustainable Energy Reviews*, *28*, 376 – 384. doi:10.1016/j.rser.2013.08.039.
- Staffell, I. (2017). Measuring the progress and impacts of decarbonising British electricity. *Energy Policy*, *102*, 463–475. doi:10.1016/j.enpol.2016.12.037.
- Staffell, I. (2019). *Electric Insights: Methodology and Sources*. Technical Report. Electric Insights. URL: https://electricinsights.co.uk/#/reports/methodology?_k=byq8ed.
- Tejada-Arango, D. A., Domeshek, M., Wogrin, S., & Centeno, E. (2018). Enhanced representative days and system states modeling for energy storage investment analysis. *IEEE Transactions on Power Systems*, *33*, 6534–6544. doi:10.1109/TPWRS.2018.2819578.
- Van der Vaart, A. W. (2007). *Asymptotic Statistics*. (8th ed.). Cambridge University Press.
- Yue, X., Pye, S., DeCarolis, J., Li, F. G. N., Rogan, F., & Ó Gallachóir, B. (2018). A review of approaches to uncertainty assessment in energy system optimization models. *Energy Strategy Reviews*, *21*, 204 – 217. doi:10.1016/j.esr.2018.06.003.
- Zeyringer, M., Price, J., Fais, B., Li, P.-H., & Sharp, E. (2018). Designing low-carbon power systems for Great Britain in 2050 that are robust to the spatiotemporal and inter-annual variability of weather. *Nature Energy*, *3*, 395–403. doi:10.1038/s41560-018-0128-x.